0026-895X/08/7301-260–269$20.00
MOLECULAR PHARMACOLOGY
Copyright © 2008 The American Society for Pharmacology and Experimental Therapeutics
Mol Pharmacol 73:260–269, 2008

Vol. 73, No. 1
41764/3290999
Printed in U.S.A.

High Mobility Group Protein B1 Is an Activator of Apoptotic Response to Antimetabolite Drugs[S]

Natalia Krynetskaia, Hongbo Xie, Slobodan Vucetic, Zoran Obradovic, and Evgeny Krynetskiy

School of Pharmacy (N.K., E.K.) and Information Science and Technology Center Biocore (H.X., S.V., Z.O.), Temple University, Philadelphia, Pennsylvania

Received September 11, 2007; accepted October 19, 2007

ABSTRACT

We explored the role of a chromatin-associated nuclear protein high mobility group protein B1 (HMGB1) in apoptotic response to widely used anticancer drugs. A murine fibroblast model system generated from *Hmgb1*$^{+/+}$ and *Hmgb1*$^{-/-}$ mice was used to assess the role of HMGB1 protein in cellular response to anticancer nucleoside analogs and precursors, which act without destroying the integrity of DNA. Chemosensitivity experiments with 5-fluorouracil, cytosine arabinoside (araC), and mercaptopurine (MP) demonstrated that *Hmgb1*$^{-/-}$ mouse embryonic fibroblasts (MEFs) were 3 to 10 times more resistant to these drugs compared with *Hmgb1*$^{+/+}$ MEFs. Hmgb1-deficient cells showed compromised cell cycle arrest and reduced caspase activation after treatment with MP and araC. Phosphorylation of p53 at Ser12 (corresponding to Ser9 in human p53) and Ser18 (corresponding to Ser15 in human p53), as well as phosphorylation of H2AX after drug treatment, was reduced in Hmgb1-deficient cells. *trans*-Activation experiments demonstrated diminished activation of proapoptotic promoters *Bax*, *Puma*, and *Noxa* in Hmgb1-deficient cells after treatment with MP or araC, consistent with reduced transcriptional activity of p53. We have demonstrated for the first time that Hmgb1 is an essential activator of cellular response to genotoxic stress caused by chemotherapeutic agents (thiopurines, cytarabine, and 5-fluorouracil), which acts at early steps of antimetabolite-induced stress by stimulating phosphorylation of two DNA damage markers, p53 and H2AX. This finding makes HMGB1 a potential target for modulating activity of chemotherapeutic antimetabolites. Identification of proteins sensitive to DNA lesions that occur without the loss of DNA integrity provides new insights into the determinants of drug sensitivity in cancer cells.

High mobility group protein B1 (HMGB1) is a versatile protein with intranuclear and extracellular functions. In the nucleus, it bends and plasticizes DNA; outside the cell, it acts as a cytokine mediator of inflammation. Despite its small size and a simple domain structure, HMGB1 facilitates numerous intranuclear processes, including transcription, replication, V(D)J recombination, and transposition (Hock et al., 2007). This versatility is achieved through the ability of HMGB1 to get involved in direct physical contacts with two distinct groups of macromolecules: HMGB1 reveals affinity with DNA cruciforms and bent, kinked, or chemically modified DNA; on the other hand, it interacts with a number of proteins, including p53, steroid hormone receptors, general and specific transcription factors, nuclear factor-κB, DNA protein kinase (DNA-PK), etc. (Bianchi and Agresti, 2005). These two distinct groups of binding substrates suggest that HMGB1 may provide a molecular link between distorted DNA, and proteins involved in DNA metabolism or genotoxic stress response. Therefore, HMGB1 is a potential modulator of anticancer therapy targeted against DNA.

Induction of apoptotic death in cancer cells via genotoxic stress by irradiation or chemotherapy remains the core of anticancer treatment. An important class of chemotherapeutic agents based on this principle, purine and pyrimidine antimetabolites, has been widely used for treatment of solid tumors and hematopoietic malignancies for several decades, although molecular triggers of apoptosis caused by these drugs remain elusive (Rich et al., 2004). For example, the

This work is supported by National Cancer Institute grant R01-CA104729 (to E.K.) and a grant from the Pennsylvania Department of Health (to Z.O.).
Article, publication date, and citation information can be found at http://molpharm.aspetjournals.org.
doi:10.1124/mol.107.041764.
[S] The online version of this article (available at http://molpharm.aspetjournals.org) contains supplemental material.

ABBREVIATIONS: HMGB1, high mobility group protein B1; DNA-PK, DNA protein kinase; FU, 5-fluorouracil; MEF, mouse embryonic fibroblast; DMEM, Dulbecco's modified Eagle's medium; MP, mercaptopurine; araC, cytosine arabinoside; MTT, 3-(4,5-dimethylthiazol-2-yl)-2,5-diphenyltetrazolium bromide; AMC, 7-amino-4-methylcoumarin; PI, propidium iodide; ATM, ataxia-telangiectasia mutated protein kinase; ATR, ataxia-telangiectasia and Rad3-related protein kinase; GAPDH, glyceraldehyde 3-phosphate dehydrogenase; PCR, polymerase chain reaction; DSB, double-strand break; H2AX and H2ax, human and murine, respectively, members of H2A histone family.

overall response rate for FU as a single agent in advanced colorectal cancer is approximately 10 to 15%, although the combination of FU with newer chemotherapies including irinotecan and oxaliplatin has improved the response rate to 40 to 50%. With approximately 2 million people treated yearly with FU, new therapeutic strategies based on better understanding of mechanisms by which these agents induce cell death are urgently needed (Longley et al., 2003).

Several antimetabolite agents do not disrupt integrity of DNA and lead only to minute alterations in DNA geometry (Sahasrabudhe et al., 1996; Somerville et al., 2003). Instead, incorporation of these chemical moieties into DNA increases local flexibility of the double helix in the area surrounding the modification, and changes the DNA-protein interactions (Krynetskaia et al., 2000; Somerville et al., 2003; Seibert et al., 2005). Early evidence that chemotherapy-induced damage in DNA alters DNA-protein interactions in chromatin came from the work of Maybaum and Mandel (1983), who described unilateral chromatid damage in cells treated with thiopurine. DNA damage-induced changes in chromatin structure are hypothesized to serve as an initiating signal in ATM genotoxic response pathway (Bakkenist and Kastan, 2003).

Earlier, we isolated a nuclear complex with increased affinity to chemotherapy-damaged DNA (Krynetski et al., 2001, 2003). An essential component of this complex is HMGB1. From our in vitro experiments, we concluded that DNA-bending protein HMGB1 plays a role of a sensor for nucleoside analogs deoxythioguanosine, deoxyfluorouridine, and cytosine arabinoside incorporated into DNA (Krynetski et al., 2001; Krynetski et al., 2003).

In contrast to other determinants of cellular sensitivity to antimetabolites, there is no known enzymatic activity for HMGB1. Here, we used a model system based on Hmgb1$^-$ knockout mouse embryonic fibroblast cells (MEFs) to elucidate the role of HMGB1 in cellular response to antimetabolite therapy. We demonstrated for the first time that HMGB1 is an essential activator of cellular response to genotoxic stress caused by chemotherapeutic agents (thiopurines, cytarabine, and 5-fluorouracil), which acts at early steps of antimetabolite-induced stress by stimulating phosphorylation of two DNA damage markers p53 and H2AX.

Materials and Methods

Cell Cultures, Drug Treatment, and Plasmids

MEFs deficient and proficient in Hmgb1 expression were generated as described previously and generously provided for this work by Dr. M. E. Bianchi (San Raffaele Scientific Institute, Milano, Italy) (Calogero et al., 1999). Cells were maintained in DMEM (Fisher Scientific, Suwanee, GA) at 40 to 80% confluence. Treatment of MEFs was performed with drugs dissolved in DMEM without serum (Fisher Scientific) as 20× stock solutions; drug concentrations [thioguanine, mercaptopurine (MP), cytarabine (araC), 5-fluorouracil (FU), cladribine, fludarabine (Sigma, St. Louis, MO), clofarabine (Genzyme, Cambridge, MA), and gemcitabine (Eli Lilly, IN)] were determined spectrophotometrically. Cell viability and cell count were determined by flow cytometry (Guava personal cell analyzer; Guava Technologies, Hayward, CA). Reporter plasmids p21-luc and pBax-luc were a generous gift from Dr. M. Oren (Weizmann Institute of Science, Rehovot, Israel), pNoxa-luc from Dr. T. Taniguchi (University of Tokyo, Tokyo, Japan), and pPuma-luc and pCMVp53 from Dr. B. Vogelstein (Johns Hopkins School of Medicine, Baltimore, MD).

Cell Growth and Chemosensitivity

Population doubling time of *Hmgb1*$^{+/+}$ and *Hmgb1*$^{-/-}$ MEFs was determined in the middle of log phase of growth. Cells were trypsinized and counted using the ViaCount protocol implemented on a Guava personal cell analyzer (Guava Technologies). Chemosensitivity was evaluated using the MTT assay (CellTiter 96 cell proliferation kit; Promega, Madison, WI) after incubation of *Hmgb1*$^{+/+}$ and *Hmgb1*$^{-/-}$ MEFs with a panel of anticancer drugs for 3 to 6 days as described previously (Carmichael et al., 1987). Cells (2×10^3 per well) were plated into 96-well plates and cultured for 3 to 6 days in the presence or absence of the following drugs: MP, thioguanine, FU, araC, cladribine, fludarabine, clofarabine, and gemcitabine. After incubation, MTT reagent was added to each well, and endpoint data were collected by a M2 microplate spectrophotometer (Molecular Devices, Sunnyvale, CA) according to the manufacturer's instructions. The IC_{50} values were calculated using Prism software (GraphPad Software Inc., San Diego, CA) by fitting a sigmoid E_{max} model to the cell viability versus drug concentration data determined in triplicate from three independent experiments.

Incorporation of Nucleoside Analogs into DNA

Hmgb1$^{+/+}$ or *Hmgb1*$^{-/-}$ cells (2×10^6) were seeded at density 25,000 cells/cm^2 and treated with [^{3}H]araC (1.6 Ci/mmol) at a final concentration of 1 μM or [^{14}C]MP (51 mCi/mmol) at a final concentration 10 μM (Moravek Biochemicals, Brea, CA). After 14 to 28 h of incubation, cells were collected by trypsinization, and DNA was extracted using DNAamp DNA Minikit (QIAGEN, Valencia, CA) according to the manufacturer's instructions. ^{3}H and ^{14}C incorporation into DNA was determined in duplicate using a Beckman LS 6500 scintillation counter (Beckman Coulter, Fullerton, CA).

Caspase Activation

Caspase activity was assessed using fluorogenic substrates for caspases 2, 3, 8, and 9 immobilized on BD Apoalert Caspase Assay plates (BD Biosciences, Palo Alto, CA). *Hmgb1*$^{+/+}$ and *Hmgb1*$^{-/-}$ MEFs were grown in DMEM and treated with 10 μM MP or 0.5 μM araC for 14, 28, or 42 h. Approximately 2×10^5 cells per sample were harvested by centrifugation and resuspended at final concentration of 2×10^5 cells/50 μl of lysis buffer. Fluorogenic substrates VDVAD-AMC (Caspase 2), DEVD-AMC (Caspase 3), IETD-AMC (Caspase 8), and LEHD-AMC (Caspase 9) were used to assay activity of corresponding caspases in cell lysates. Actinomycin D (0.5 μg/ml) was used as a positive control. The plates were analyzed using a fluorescence microplate reader M2 (Molecular Devices), and caspase activity was normalized per milligram of total protein. Each experiment was performed in triplicate.

Cell Cycle Analysis

For cell cycle analysis, cells were trypsinized, centrifuged, and resuspended at a concentration of 1×10^6/ml in a propidium iodide (PI) staining solution (0.05 mg/ml PI, 0.1% sodium citrate, and 0.1% Triton X-100). Each sample was treated with DNase-free RNase (5 ng/ml; Calbiochem, San Diego, CA) at room temperature for 30 min, filtered through 40-μm mesh, and analyzed by a FACScan flow cytometer (Becton Dickinson, San Jose, CA) collecting the fluorescence (wavelength range, 563–607 nm) from PI-bound DNA (approximately 15,000 cells). The percentages of cells within each phase of the cell cycle were computed by using ModFit software (Verity Software House, Topsham, ME).

Transfection of MEFs

Approximately 2.5×10^4 cells per well were seeded in 24-well plates and transfected with plasmids containing *Luc* gene under control of *p21*, *Bax*, *Puma*, or *Noxa* promoters and TP53 gene under control of cytomegalovirus promoter using FuGene 6 transfection reagent (Roche, Indianapolis, IN). The next day, cells were treated with 10 μM MP or 0.5 μM araC and incubated for 28 h. After

incubation, cells were lysed and stored at −20°C until analysis. Luciferase activity was measured using a Dual-Luciferase Reporter Assay Kit (Promega), as indicated in the manufacturer's instructions. Data were collected from a 96-well plate by Clarity luminescence microplate reader (Bio-Tek Instruments, Winooski, VT). The expression of the promoter-driven firefly luciferase was normalized using the activity of constitutively expressed *Renilla reniformis* luciferase (Promega).

For HMGB1 expression experiments, Hmgb1$^{-/-}$ MEFs were transfected with pCMV-SPORT6 plasmid with human HMGB1 cDNA insert (clone 1F5; Open Byosystems, Huntsville, AL). Control cells were transfected with a vector without HMGB1 cDNA. Transfection was performed with FuGene 6 transfection reagent (Roche) as described above. Two days after transfection, the cells were treated with 10 μM MP, incubated for 42 h, and collected for Western blot analysis.

Western blot analysis was performed as described previously (Krynetski et al., 2003). In brief, 5×10^6 control cells and cells after drug treatment were rinsed with ice-cold phosphate-buffered saline, lysed with triple detergent lysis buffer and scraped off the plates; lysates were sonicated four times for 5 s each on ice and centrifuged in the microtubes for 10 min at 4°C. Concentration of protein in supernatant was determined by PlusOne 2-D Quant kit (GE Healthcare, Little Chalfont, Buckinghamshire, UK). Forty micrograms total protein was loaded onto 12% polyacrylamide gel and transferred to a polyvinylidene difluoride or a nitrocellulose membrane (Invitrogen, Carlsbad, CA) in a Mini Trans-Blot electrotransfer cell (Bio-Rad Laboratories, Hercules, CA). Membranes were developed with primary antibodies specific to p53 and p53 phosphorylated at Ser12 and Ser18 (Cell Signaling, Danvers, MA), γ-H2AX (H2AX phosphorylated at Ser139) (Upstate, Charlottesville, VA), ATM phosphorylated at Ser1981 (Abcam, Inc., Cambridge, MA), and ATR (Santa Cruz Biotechnology, Santa Cruz, CA). Anti-GAPDH antibody (Chemicon, Temecula, CA) and β-actin (Sigma) were used for loading controls. For detection of ATM and ATR proteins, protein extract was separated using 7% Tris-acetate gels (Invitrogen). Bands were visualized and quantified by PhosphorImager with the ImageQuaNT Software system (GE Healthcare), using blue fluorescence/chemifluorescence at 488 nm excitation, or Odissey Infrared Imaging system (LI-COR BioSciences, Lincoln, NE) using two-color fluorescence detection at 700 and 800 nm.

Gene Expression Experiments

Total cellular RNA was extracted with TriReagent (Invitrogen) from untreated *Hmgb1*$^{+/+}$ and *Hmgb1*$^{-/-}$ MEFs (approximately 5×10^6 cells per experiment, seven replicates) and used for reverse transcription PCR and DNA microarray experiments.

Analysis of *Atm and Atr* Expression by Real-Time PCR. Approximately 500 ng of total RNA was reverse-transcribed using the TaqMan Reverse Transcription kit (Applied Biosystems, Foster City, CA) according to manufacturer's instructions. The level of Atm and Atr mRNA was evaluated using relative quantification protocol with murine β-actin as a normalization standard on a real-time PCR instrument (ABI 7300; Applied Biosystems) according to manufacturer's instructions. Data were collected from three independent experiments for each sample.

DNA Microarray Study. Total RNA was processed and hybridized to the GeneChip Murine Genome U74Av2 oligonucleotide microarray (Affymetrix, Santa Clara, CA) containing 12,489 probe sets per manufacturer's instructions. For each experiment, consistency among replicate arrays was evaluated by measuring correlation coefficients among any given two chips' (X,Y) intensity readings.

$$\text{Correlation coefficient} = \frac{\sum_{i=1}^{n} (\dot{x}_i - \bar{x})(y_i - \bar{y})}{\sum_{i=1}^{n}(x_i - \bar{x}) \times \sum_{i=1}^{n}(y_i - \bar{y})}$$

where $\bar{x}$ is mean intensity value of all genes in chip X, $\bar{y}$ is mean intensity value of all genes in chip Y, x_i is intensity reading of gene$_i$ in chip X, and y_i is intensity reading of gene$_i$ in chip Y. Matlab function "corrcoef" was used to measure correlation coefficient of two arrays' intensities. A correlation coefficient value close to "1" between two arrays was considered indicative of good consistency of replicates, whereas a value of "0" implied no correlation at all (Xie et al., 2007).

Selection of Differentially Expressed Genes

Gene expression values were extracted using the Affymetrix Microarray Suite version 5.0. In the experiment (*Hmgb1*$^{+/+}$ versus *Hmgb1*$^{-/-}$ MEFs), genes differentially expressed in untreated *Hmgb1*$^{+/+}$ and *Hmgb1*$^{-/-}$ MEFs were defined as genes that had 1) >2-fold difference between the cells and 2) had a P value for the t test <0.05 (Bolstad et al., 2003). Before statistical analysis, gene expression data were normalized using the quantile normalization method (Bolstad et al., 2003). Data quality in gene expression experiments was evaluated by calculating correlation coefficients among all arrays with *Hmgb1*$^{+/+}$ and *Hmgb1*$^{-/-}$ MEFs (Xie et al., 2007). Gene expression values (log ratio) of selected genes were analyzed by hierarchical clustering analysis implemented in Spotfire statistical software (Spotfire, Somerville, MA).

Bioinformatics Analyses and Ontology Classification of Discriminative Genes

Selected genes were imported into Ingenuity software to identify gene networks that are particularly enriched with the selected genes by searching against Ingenuity global molecular network (Ingenuity Systems, Redwood City, CA). Pathway annotations of genes were obtained from the Affymetrix (Santa Clara, CA) annotation file. Fisher's exact test (Ben-Shaul et al., 2005) was used to examine whether the selected differentially expressed genes were overrepresented within a given pathway.

Statistical Analysis. Data are presented as the mean ± S.E. The statistical analyses were carried out using Student's t test with Statistica software (StatSoft, Tulsa, OK). A P value <0.05 was considered statistically significant.

Results

Hmgb1-Deficient MEFs Demonstrated Delayed Cytotoxicity after Treatment with Anticancer Genotoxic Drugs

Under conditions of experiments, the growth rates of Hmgb1-deficient and -proficient cells were similar: population doubling times in the middle of exponential phase for *Hmgb1*$^{+/+}$ and *Hmgb1*$^{-/-}$ MEFs were 14.4 and 15.7 h, respectively. Chemosensitivity to a panel of anticancer drugs (nucleoside analogs and their precursors) was assessed in *Hmgb1*$^{+/+}$ and *Hmgb1*$^{-/-}$ MEFs (Table 1 and Fig. 1S). Hmgb1-deficient cells revealed 3 to 10 times higher viability by MTT assay after 3 to 6 days' incubation with FU, araC, thioguanine, and MP, although there was marginal or no difference in chemosensitivity of *Hmgb1*$^{+/+}$ and *Hmgb1*$^{-/-}$ MEFs treated with cladribine, clofarabine, fludarabine, and gemcitabine (Table 1). Actual proliferation plots are given in the Supplemental Materials (Fig. 1S). These results were consistent with our previous data on relative resistance of Hmgb1-deficient cells to thiopurines (Krynetski et al., 2003). MP, araC, and FU were used in subsequent experiments to elucidate the role of HMGB1 in cell death after anticancer drug treatment.

Incorporation of radiolabeled nucleoside analogs araC and deoxythioguanosine (the product of metabolic activation of

MP) into DNA occurred at similar levels in both cell lines (*Hmgb1*$^{+/+}$ and *Hmgb1*$^{-/-}$ MEFs, $P = 0.78$), irrespective of the status of Hmgb1 (Fig. 2S).

TABLE 1

Effect of chemotherapeutic agents on MEF cell viability (IC_{50})

MEF (*Hmgb1*$^{+/+}$ vs. *Hmgb1*$^{-/-}$) were incubated with different drug concentrations for 5 days, and viability was measured by MTT assay. Each value is the mean of three replicates ± S.D. ($P < 0.05$).

Drug	IC_{50}[a]	
	Hmgb1$^{+/+}$ MEF	*Hmgb1*$^{-/-}$ MEF
	μM	
Mercaptopurine	0.8 ± 0.12	8.9 ± 0.65
Thioguanine	0.5 ± 0.11	2.2 ± 0.29
Cytarabine	0.4 ± 0.02	1.7 ± 0.08
Fluorouracil	1.3 ± 0.35	6.2 ± 0.17
Fludarabine	2.9 ± 0.13	4.3 ± 0.21
Cladribine	1.9 ± 0.29	2.91 ± 0.16
Gemcitabine	0.02 ± 0.001	0.02 ± 0.005
Clofarabine	0.6 ± 0.15	0.7 ± 0.07

Caspase Activation after Drug Treatment Was Reduced in Hmgb1-Deficient Cells

To gain further insight into cytotoxic effects of anticancer nucleosides in relation to Hmgb1 functions, we compared activity of apoptotic markers (caspases 2, 3, 8, and 9) in *Hmgb1*$^{+/+}$ and *Hmgb1*$^{-/-}$ cells. Caspase activation was monitored using fluorogenic substrates after treatment with MP and araC for 14 to 42 h. After treatment of *Hmgb1*$^{+/+}$ cells with 10 μM MP or 0.5 μM cytarabine for 42 h, we detected 8- to 12-fold activation of caspases 2 and 3 in *Hmgb1*$^{+/+}$ cells (Fig. 1A, open columns) versus 2- to 4-fold activation in *Hmgb1*$^{-/-}$ cells (Fig. 1A, black columns), thus confirming the induction of the apoptotic cascade after the genotoxic stress. It is noteworthy that activation of caspases 2 and 3 was significantly lower in *Hmgb1*$^{-/-}$ cells compared with *Hmgb1*$^{+/+}$ cells, suggesting a key role of Hmgb1 in induction of apoptosis in response to antimetabolite nucleoside analogs. In contrast, activation of caspases 8 and 9 after araC treatment for 42 h in Hmgb1-proficient cells was less pronounced (1.5- to 2-fold) albeit still significantly higher

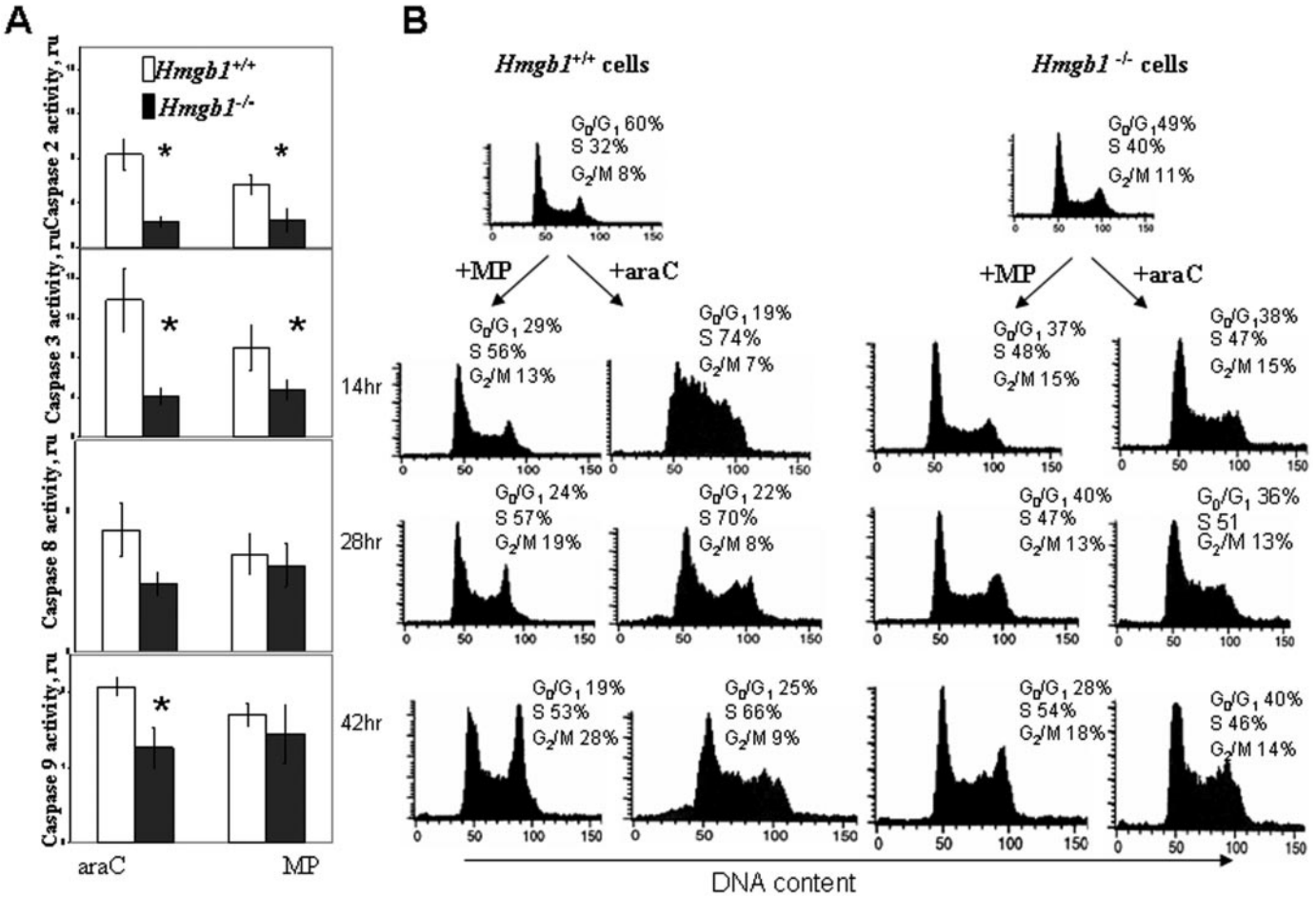

Fig. 1. Hmgb1-deficient cells demonstrate decreased caspase activity and compromised cell cycle arrest after genotoxic stress induced by antimetabolite drugs. A, activation of caspases 2, 3, 8, and 9 in *Hmgb1*$^{+/+}$ MEFs compared with *Hmgb1*$^{-/-}$ MEFs after 42 h of treatment with 10 μM MP or 0.5 μM araC. Activity of caspases was assayed using fluorogenic substrates as described under *Materials and Methods*. Relative activity of individual caspases in treated cells was expressed as a ratio to caspase activity in untreated cells after normalization per milligram of protein. Data are the mean ± S.D. generated from three independent experiments. *ru*, relative units. Asterisks denote significantly different levels of activity ($P < 0.05$). B, cell cycle arrest is induced by anticancer drugs in *Hmgb1*$^{+/+}$ but not in *Hmgb1*$^{-/-}$ MEFs. *Hmgb1*$^{+/+}$ (right) and *Hmgb1*$^{-/-}$ (left) MEFs were treated with 10 μM MP and 0.5 μM araC for 14, 28, and 42 h, stained with propidium iodide, and DNA content was analyzed using flow cytometry after treatment with DNase-free RNase. The percentages of *Hmgb1*$^{+/+}$ and *Hmgb1*$^{-/-}$ cells in G_0/G_1, S, and G_2-M phases were determined by DNA histogram analysis.

than in Hmgb1-deficient cells. Difference in caspase 8 and caspase 9 activation after MP treatment did not reach significance (Fig. 1A).

Treatment with Anticancer Drugs MP and araC Interrupted Cell Cycle Progression in *Hmgb1*$^{+/+}$ but Not in *Hmgb1*$^{-/-}$ Cells

We set up experiments to assess the effect of Hmgb1 status on cell cycle progression. Treatment of asynchronous *Hmgb1*$^{+/+}$ MEFs with 10 μM MP for 14 to 42 h resulted in cell cycle arrest in G_2/M phase (28% of treated cells versus 8% of untreated cells after 42 h of incubation) with a concomitant decrease of cells in G_0/G_1 phase (19% of treated cells versus 60% of untreated cells). On the other hand, in *Hmgb1*$^{-/-}$ cells, this effect was less pronounced (18% of treated cells versus 11% in untreated cells in G_2/M phase after 42 h of incubation) (Fig. 1B). Treatment of *Hmgb1*$^{+/+}$ MEFs with 0.5 μM araC resulted in cell cycle arrest in S phase after the first cell division. The percentage of *Hmgb1*$^{+/+}$ cells in S phase increased from 32 to 74% after 14 h of treatment and remained at 70% after 28 h of incubation (Fig. 1B). In *HMGB1*$^{-/-}$ MEFs, the percentage of cells in S phase increased from 40 to 47% after 14 h of incubation with araC (Fig. 1B). These results support our hypothesis that Hmgb1 modulates the cellular response to antimetabolite nucleoside analogs.

Hmgb1 Modulated Phosphorylation of p53 and H2AX Proteins after Treatment with Genotoxic Chemotherapeutic Drugs MP, FU, and araC

Accumulation of Ser12- and Ser18-Phosphorylated p53. Transcriptional activation of p53 protein after DNA damage is accompanied by a series of post-translational modifications, among which phosphorylation of Ser15 is thought to be the initial event in a series of subsequent modifications leading to stabilization and biochemical activation of p53 (Meek, 2004). We compared post-translational modification of p53 in *Hmgb1*$^{+/+}$ and *Hmgb1*$^{-/-}$ cells in response to genotoxic stress caused by treatment with MP, araC, and FU. To monitor the status of p53, we used antibodies to phosphorylated forms of p53 (Soubeyrand et al., 2004). Ser9 and Ser15 in human p53 are evolutionarily conserved residues, corresponding to Ser12 and Ser18 in murine p53; these residues can be phosphorylated by several protein kinases including ATM, ATR, and DNA-PK (Chao et al., 2003). After treatment of murine cells with 10 μM MP, 0.5 μM araC, and 10 μM FU, we observed accumulation of strong signals corresponding to p53 phosphorylated at Ser12 and Ser18 in Hmgb1-proficient cells. In contrast to Hmgb1-proficient cells, phosphorylation of p53 in Hmgb1-deficient cells was 6- to 8-fold decreased, and accumulation of phospho-Ser12 and phospho-Ser18 occurred at lower rate (Figs. 2A and 3A). A general inhibitor of phosphoinositide-3-kinase-related protein kinase family-like kinases, wortmannin, decreased phosphorylation of Ser18, suggesting that one of the DNA damage-activated kinases ATM, ATR, or DNA-PK catalyze phosphorylation of p53 after drug treatment (data not shown). Treatment of cells at two concentrations of drug (0.8 and 10 μM MP) revealed that the level of phosphorylated product paralleled drug concentration (Fig. 2B).

Accumulation of γ-H2ax. After the generation of DSB after replication stress, genotoxic insult, or other stimuli, a network of PIKK-like kinases is activated, causing rapid phosphorylation of histone H2AX at C-terminal Ser139 residue (Fernandez-Capetillo et al., 2004). Thus, accumulation of γ-H2AX (a phosphorylated form of H2AX) is a strong indicator of DSB formation. Using antibody specific to H2AX phosphorylated at Ser139, we evaluated accumulation of DSB after treatment with MP, araC, and FU. Similarly to Ser12- and Ser18-phosphorylated forms of p53, accumulation of γ-H2ax after drug treatment was detected after 14 to 42 h

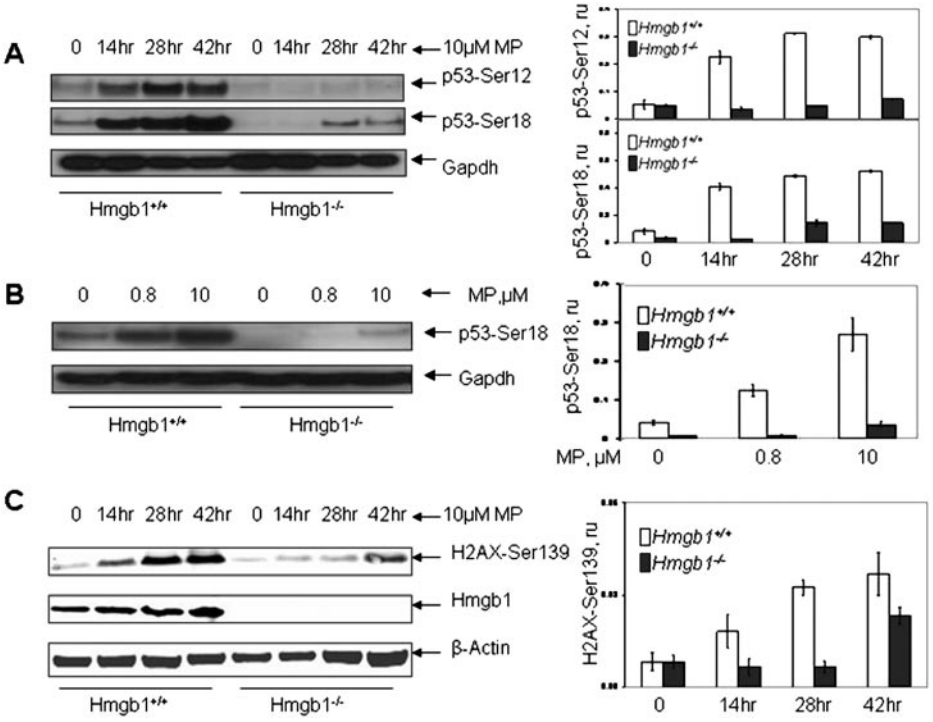

Fig. 2. Phosphorylation of p53 and H2ax proteins in MEFs with different Hmgb1 status after MP treatment. A, Western blotting analysis of p53 phosphorylation at Ser12 and Ser18 (left) and relative levels of p53 phosphorylation normalized versus GAPDH (right). B, induction of Ser18 phosphorylation in p53 increases with increased concentration of MP in both cell lines after 28 h of treatment. C, Western blotting analysis of H2ax phosphorylation at Ser139 (left) and relative levels of H2ax phosphorylation normalized versus β-actin (right). Cells were treated with 10 μM MP for 14 to 42 h. Lysates from untreated cells were used as control. Analysis with anti-Hmgb1 antibody (B, the central strip) confirmed the cell phenotype. 0, no drug treatment (control). Data are expressed as the mean $\pm$ S.D. of three independent experiments. Bars, SD. *ru*, relative units.

of incubation in Hmgb1-proficient MEFs (Figs. 2C and 3B). It is noteworthy that the level of γ-H2ax after MP, araC, and FU treatment was significantly reduced in Hmgb1-deficient cells, indicating a functional role of Hmgb1 in response to drug treatment. The accumulation of γ-H2ax occurred at different rates for the three drugs: after MP treatment of $Hmgb1^{+/+}$ MEFs, the phosphorylated product was detectable after 14 h and reached the maximum level after 42 h of incubation. In contrast, the maximum level of γ-H2ax was achieved after 14 h of incubation with FU and 28 h of incubation with araC, correspondingly. In $Hmgb1^{-/-}$ cells treated with MP, araC, and FU, the accumulation of Ser139-phosphorylated product reached maximal level after 42 h (the third cycle of cell division), indicating delayed response in comparison with $Hmgb1^{+/+}$ cells.

At least three PIKK family members, ATM, ATR, and DNA-PK, catalyze phosphorylation of Ser139 in H2AX. There is functional redundancy among the pathways because H2AX phosphorylation remains detectable in $ATM^{-/-}$, $DNA\text{-}PK^{-/-}$, and $ATR^{-/-}$ knockout cells (Fernandez-Capetillo et al., 2004). Using real-time PCR technique, we evaluated the relative level of Atm and Atr mRNA in $Hmgb1^{+/+}$ and $Hmgb1^{-/-}$ MEFs. Our experiments revealed approximately 2.5-fold higher Atm mRNA expression in $Hmgb1^{+/+}$ cells compared with $Hmgb1^{-/-}$ cells ($P < 0.001$); Atr mRNA was slightly (1.2 times) overexpressed in $Hmgb1^{+/+}$ cells compared with $Hmgb1^{-/-}$ cells. This difference did not reach statistical significance ($P = 0.057$). At the protein level, the increase of an active form of ATM phosphorylated at Ser1981 after treatment with 10 μM MP was not significant (Fig. 3S, A and B). In contrast, Western analysis revealed increased level of Atr protein in $Hmgb1^{+/+}$ cells after 28 h of incubation with MP (Fig. 3S, A and C).

Hmgb1 Stimulated *trans*-Activation of p53-Regulated Pro-Apoptotic Promoters in Cells Treated with Chemotherapeutic Drugs MP and araC

Because chemotherapeutic agents used in this study (FU, araC, and MP) are known to exert their cytotoxic effect via the p53-mediated pathway (Bunz et al., 1999; Zhang et al., 2000, 2007; Yin et al., 2006), we used luciferase reporter plasmids to assess the role of Hmgb1 in transcriptional activity of p53 after genotoxic stress. $Hmgb1^{+/+}$ and $Hmgb1^{-/-}$ MEFs were transfected with *Luc*-expressing reporter plasmids driven by p53-regulated promoters (*p21*, *Bax*, *Puma*, and *Noxa*) and then treated with anticancer drugs MP and araC. After 28 to 42 h of incubation with 10 μM MP and 0.5 μM araC, we observed an increased luciferase expression driven by p53-regulated promoters indicative of induction of p53 transcriptional activity (Fig. 4). In particular, proapoptotic promoters *Puma* and *Noxa* were 2- to 3-fold more active in $Hmgb1^{+/+}$ than in $Hmgb1^{-/-}$ MEFs in response to genotoxic stress after MP treatment. After treatment with araC, three reporter plasmids (pBax-*luc*, pPuma-*luc*, and pNoxa-*luc*) revealed significantly increased promoter activity (4–8-fold) in $Hmgb1^{+/+}$ compared with $Hmgb1^{-/-}$ MEFs, although activity of p21 promoter did not differ significantly in these two cell lines (Fig. 4).

Transient Expression of Human HMGB1 Rescued Phosphorylation of p53 and H2ax in Hmgb1 Knockout Cells

We examined whether re-expressing HMGB1 in Hmgb1-knockout murine cells restores phosphorylation of p53 and H2ax after genotoxic stress caused by drug treatment. Transfection of $Hmgb1^{-/-}$ MEFs with human HMGB1 cDNA

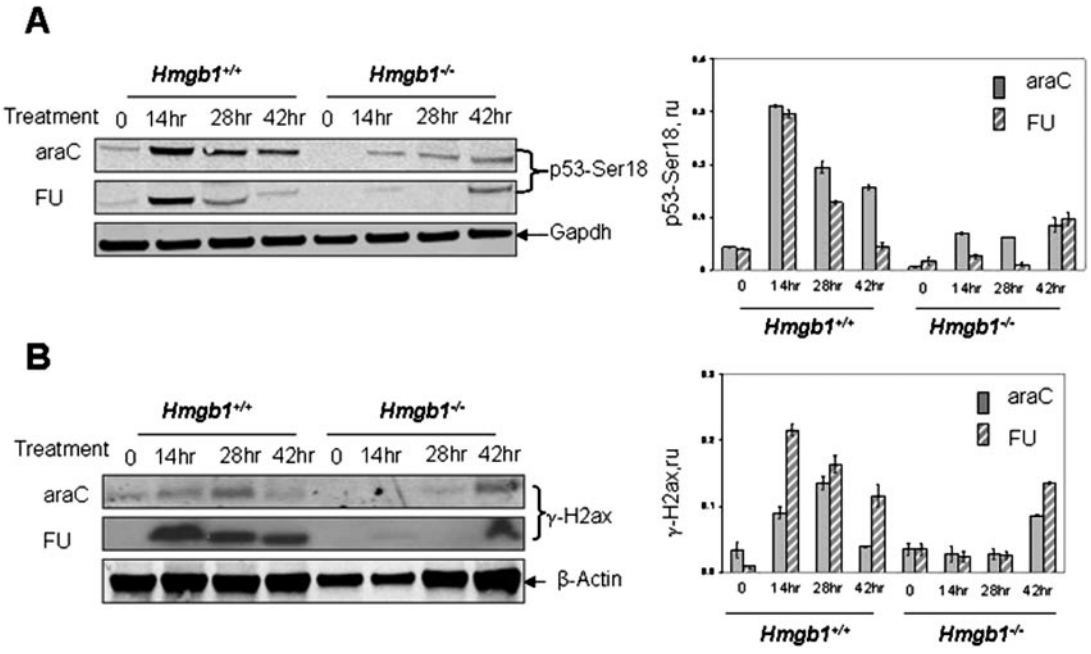

Fig. 3. Phosphorylation of p53 and H2ax proteins in MEFs with different Hmgb1 status after araC and FU treatment. A, Western blotting analysis of N-terminal phosphorylation of p53 at Ser18 (left) and relative levels of p53 phosphorylation normalized versus GAPDH for both drugs (right). B, Western blotting analysis of H2ax phosphorylation at Ser139 after treatment with araC and FU (left), and relative levels of H2ax phosphorylation normalized versus β-actin for both drugs (right). Cells were treated with 0.5 μM araC or 10 μM FU for 14 to 42 h. Lysates from untreated cells were used as a control. Data are expressed as the mean ± S.D. of three independent experiments. Bars, S.D. *ru*, relative units. 0, no drug treatment (control).

driven by cytomegalovirus promoter resulted in accumulation of HMGB1 in the cells (Fig. 5). After treatment with 10 μM MP for 28 h, we observed increased accumulation of p53 phosphorylated at Ser18, and H2ax phosphorylated at Ser139 in *Hmgb1*$^{-/-}$ cells transfected with HMGB1 cDNA, compared with cells transfected with the control plasmid (Fig. 5).

Microarray Experiments Revealed Distinct Gene Regulation Patterns Depending on Hmgb1 Status of Cells

Using total RNA extracted from *Hmgb1*$^{+/+}$ and *Hmgb1*$^{-/-}$ MEFs in seven independent experiments, we compared gene expression patterns in these two cell lines using DNA microarray technology. All replicates had a correlation coefficient value >0.90, which indicated good quality of collected data. Forty-five probe sets representing 43 genes had at least 2-fold higher expression levels in Hmgb1-proficient MEFs compared with Hmgb1-deficient MEFs and formed tight clusters by hierarchical clustering analysis (Fig. 6A). *Hmgb1* gene was identified as one gene having the highest discriminative ratio, thus confirming the accuracy of collected data.

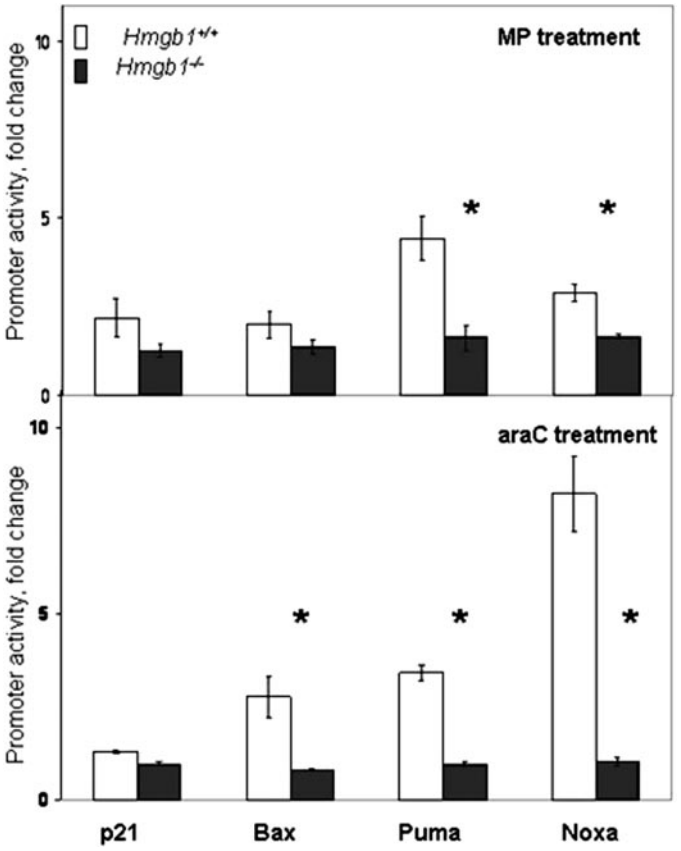

Fig. 4. HMGB1 contributes to activation of p53 target genes in response to genotoxic stress. *Hmgb1*$^{+/+}$ and *Hmgb1*$^{-/-}$ MEFs were transfected with luciferase reporter plasmids driven by *p21*, *Bax*, *Puma*, and *Noxa* promoters, or control plasmid, and treated with 10 μM MP (upper panel) or 0.5 μM araC (lower panel). Trans-activation of p53-regulated promoters *p21*, *Bax*, *Puma*, and *Noxa* in MEFs was normalized by constitutively expressed *R. reniformis* luciferase activity. Activity of *Puma* and *Noxa* promoters was significantly different in two cell lines after MP treatment, and activity of *Bax*, *Puma*, and *Noxa* promoters was significantly different after araC treatment ($P < 0.05$). Results of experiments are depicted as -fold change of promoter activity relative to cells untreated with genotoxic drugs. Data are expressed as the mean ± S.D. of three independent experiments. Asterisks denote significantly different levels of activity ($P < 0.05$). Bars, S.D.. *ru*, relative units.

Identification of gene networks enriched with the selected genes using the Ingenuity algorithm elucidated several pathways dependent on the Hmgb1 status of cells (Fig. 6B). In particular, genes involved in intracellular signaling pathways, cell cycle pathway, and apoptosis were differentially expressed in *Hmgb1*$^{+/+}$ compared with *Hmgb1*$^{-/-}$ ($P < 0.05$ by Fisher's exact test). This finding parallels our data indicating the role of Hmgb1 in induction of apoptosis. The complete list of genes differentially expressed in *Hmgb1*$^{+/+}$ versus *Hmgb1*$^{-/-}$ cells is provided in Supplementary Table S1. These data suggest that architectural transcription factor Hmgb1 is involved in regulation of several important pathways and may contribute to modulation of therapeutic efficacy of antimetabolite chemotherapeutic agents.

Discussion

Cellular response to DNA damage relies on recognition of structural elements such as double-strand breaks, abnormal nucleobases, or apurinic sites, to name just a few. On the other hand, DNA damage sensors may respond to dynamic changes in DNA (e.g., DNA bending) rather than static structural features (Seibert et al., 2005).

In this study, we used a murine fibroblast model system generated from *Hmgb1*$^{+/+}$ and *Hmgb1*$^{-/-}$ mice to assess the role of the DNA-bending protein HMGB1 in cell sensitivity to antimetabolite nucleoside analogs. Our results suggest a mechanistic explanation to increased resistance of Hmgb1-deficient cells to chemotherapeutic agents: induction of p53-mediated apoptosis by chemotherapeutic agents was evidently compromised in Hmgb1-deficient cells. This conclusion is supported by several lines of evi-

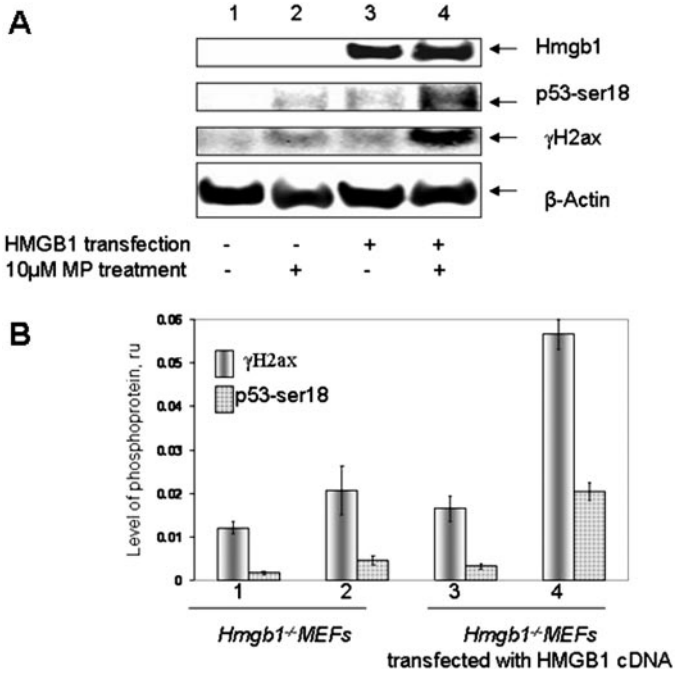

Fig. 5. Expression of human HMGB1 restores phosphorylation of p53 and H2ax in Hmgb1 knockout MEFs. A, accumulation of Ser18-phosphorylated p53 and γ-H2ax in *Hmgb1*$^{-/-}$ cells transfected with human HMGB1-expressing plasmid and treated with 10 μM MP for 28 h. Expression of HMGB1 in *Hmgb1*$^{-/-}$ MEFs is shown on the top strip; β-actin, loading control. B, relative levels of phosphorylation of p53 at Ser18 and H2ax at Ser139 after MP treatment of mock- and HMGB1-transfected cells. β-Actin was used for normalization of signals.

dence: first, Hmgb1-deficient cells are more resistant to antimetabolite agents FU, araC, and MP (Table 1) despite comparable incorporation of nucleoside analogs into DNA (Fig. 2S); second, caspase activation is reduced in Hmgb1-deficient MEFs, compared with Hmgb1-proficient cells (Fig. 1A); third, Hmgb1-deficient cells manifest a defect in cell cycle arrest after drug treatment (Fig. 1B); fourth, *trans*-activation experiments demonstrate diminished activation of pro-apoptotic promoters *Bax*, *Puma*, and *Noxa* in Hmgb1-deficient cells (Fig. 2); fifth, phosphorylation of DNA damage markers p53 and H2AX is reduced in Hmgb1-deficient cells (Figs. 3 and 4); and sixth, re-expression of HMGB1 in Hmgb1 knockout cells restores phosphorylation of p53 and H2ax (Fig. 5).

The incorporation of nucleoside analogs is similar in $Hmgb1^{+/+}$ and $Hmgb1^{-/-}$ cells, indicating that metabolic activation of genotoxic drugs occurs at comparable levels in these two cell lines. The two drugs used in incorporation experiments (araC and MP) are metabolically activated through two different pathways (i.e., the nucleoside phosphorylation and purine salvage pathways, respectively). Nevertheless, the effect of Hmgb1 abrogation is similar for these drugs, suggesting that Hmgb1 exerts its action after the nucleoside analogs are incorporated into DNA.

Because antimetabolites act via several complementary mechanisms, it is difficult to attribute their effects to genotoxicity versus alternative ways of action (e.g., inhibition of metabolic reactions). The use of gene-targeted cell lines where specific steps in DNA repair or DNA damage response are changed proves to be instrumental in discriminating between metabolic and genotoxic mechanisms of action. Using cells deficient in base excision repair, An et al. (2007) demonstrated that incorporation of fluorouracil in DNA is the predominant cause of FU cytotoxicity. In our experiments, we used murine cells deficient in Hmgb1 protein, which is not known to participate in drug metabolism or anabolic activation of drugs. Instead, this protein plays an important role in maintenance of nucleosome structure and regulation of gene transcription (Yamada and Maruyama, 2007). Therefore, changes in chromatin architecture or gene regulation patterns could be important determinants of antimetabolite therapy.

A

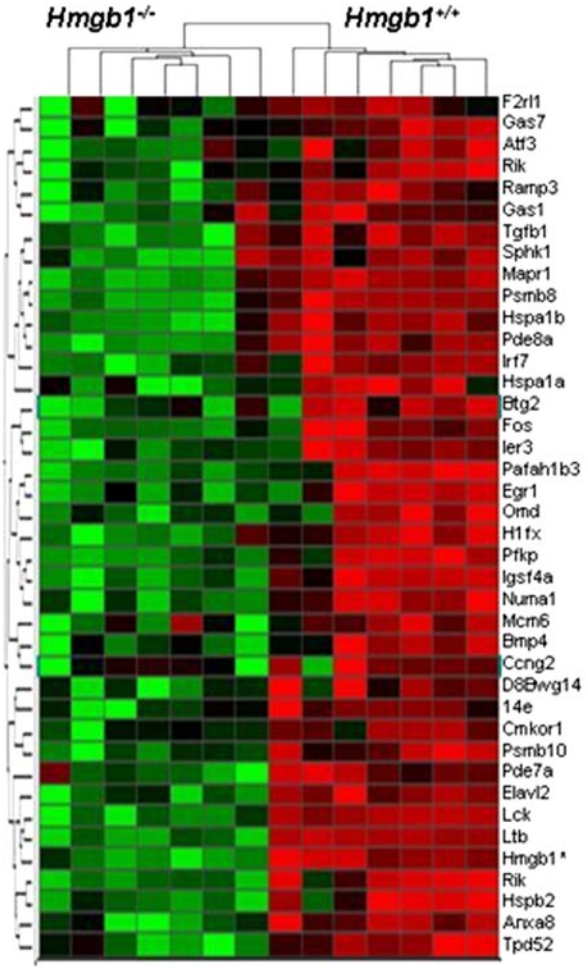

B

Pathway	p-value
TGF_Beta_Signaling_Pathway	0
Smooth_muscle_contraction	0.0007
Proteasome_Degradation	0.0019
Cell_Cycle_KEGG	0.004
G_Protein_Signaling	0.0067
Fructose and mannose metabolism	0.01
Galactose metabolism	0.01
Ovarian_Infertility_Genes	0.0104
Prostaglandin_synthesis_regulation	0.0109
DNA_replication_Reactome	0.0156
Glycolysis_and_Gluconeogenesis	0.0203
Purine metabolism	0.0203
Inflammatory_Response_Pathway	0.0216
Apoptosis	0.0459
mRNA_processing_binding_Reactome	0.1379

Fig. 6. Discriminative genes differently expressed in untreated $Hmgb1^{+/+}$ versus $Hmgb1^{-/-}$ MEFs. A, hierarchical clustering analysis of discriminative genes highly expressed in $Hmgb1^{+/+}$ cells compared with $Hmgb1^{-/-}$ cells (red channel, overexpressed; green channel, underexpressed). Total RNA from two cell lines was extracted and hybridized with Affymetrix microarray chips in seven independent experiments; tight clusters of $Hmgb1^{+/+}$ versus $Hmgb1^{-/-}$ cells indicate that the gene expression profiles in these two cell lines are essentially different. Supplemental Table S1 contains the complete list of discriminative genes. B, over-represented functional categories within gene clusters regulated by Hmgb1. Pathways containing significantly differentially expressed genes in $Hmgb1^{+/+}$ versus $Hmgb1^{-/-}$ MEFs were identified by Fisher exact test ($P < 0.05$).

Structural analysis of synthetic DNA showed that incorporation of nucleoside analogs into DNA does not introduce gross changes in DNA geometry (Sahasrabudhe et al., 1996; Somerville et al., 2003). Instead, drastic shifts in DNA dynamics occur; for example, incorporation of deoxythioguanosine makes DNA more flexible (Somerville et al., 2003). Although introduction of a kink into perfect DNA is thermodynamically unfavorable, the presence of elements that enhance DNA flexibility facilitates DNA bending (Lorenz et al., 1999). The increased DNA flexibility can be detected by DNA-bending proteins and interpreted as a genotoxic insult, thus providing the primary signal for activation of DNA damage response.

Multiple in vitro and clinical studies provided evidence that antimetabolites act via the p53-mediated apoptotic pathway, which includes phosphorylation and transcriptional activation of p53 (Bunz et al., 1999; Zhang et al., 2000; Decker et al., 2003; Longley et al., 2003; Kaeser et al., 2004; Yin et al., 2006). In our experiments, we found that MP, araC, and FU induced Ser12 and Ser18 phosphorylation in murine p53. Analysis performed over a range of MP concentrations (i.e., at IC_{50} for wild-type and knockout MEFs) demonstrated increased phosphorylation of p53 with increasing drug concentrations. At both drug concentrations, phosphorylation of p53-Ser12 and p53-Ser18 in Hmgb1-deficient cells was significantly lower, suggesting that Hmgb1 acts in the beginning of the p53-mediated stress response. In parallel, transcriptional activity of p53-regulated pro-apoptotic promoters was decreased in Hmgb1-knockout cells. Another marker of genotoxic stress used in this study was γ-H2ax, which is a strong indicator of DSB formation as a result of various genotoxic insults, or during the execution phase of apoptosis (Rogakou et al., 2000; Hanasoge and Ljungman, 2007). Similarly to Ser12- and Ser18-phosphorylated form of p53, accumulation of γ-H2ax was significantly reduced in Hmgb1-knockout cells.

Ectopic expression of human HMGB1 in murine Hmgb1-knockout cells restored phosphorylation of p53 and H2ax, thus confirming the functional role of Hmgb1 in genotoxic stress response. Human HMGB1 protein differs in only one amino acid residue from the murine Hmgb1 protein and evidently can rescue at least some of its functions.

Phosphorylation of Ser15 in p53 and phosphorylation of Ser139 in H2AX are catalyzed by one or more of the PIKK-like protein kinases, ATM, ATR, or DNA-PK (Meek, 2004). Taken together, the reduced phosphorylation of p53 and H2ax markers in $Hmgb1^{-/-}$ MEFs indicates that the activity of one of these kinases depends on Hmgb1 status of the cells. Gene and protein expression data suggest that this may occur at different levels: transcription of the *Atm* gene was 2.5-fold higher in untreated Hmgb1-proficient compared with Hmgb1-deficient cells, as revealed by reverse transcription PCR. We observed a trend to the increase of activated Atm (phosphorylated at Ser1981) in $Hmgb1^{+/+}$ rather than $Hmgb1^{-/-}$ cells after drug treatment, although the difference did not reach significance (Fig. 3S, A and B). On the other hand, *Atr* transcription was similar in untreated $Hmgb1^{+/+}$ and $Hmgb1^{-/-}$ cells. It is noteworthy that after 28 to 42 h of exposure to MP, increased level of Atr protein was detected in Hmgb1-proficient but not Hmgb1-deficient cells; this observation suggests that Hmgb1 could augment Atr synthesis or stability under conditions of genotoxic stress (Fig. 3, A and C).

On the other hand, abrogation of protein-protein interaction between Hmgb1 and p53 or H2ax in $Hmgb1^{-/-}$ cells could inhibit phosphorylation of p53 and H2ax. Several in vitro studies have examined HMGB1-p53 interaction and demonstrated that HMGB1 enhances p53 sequence-specific DNA binding by a mechanism involving structural changes in the target DNA (Jayaraman et al., 1998; Imamura et al., 2001; McKinney and Prives, 2002). No data on HMGB1-H2AX interactions have been reported thus far. At present, this second scenario cannot be excluded and merits experimental testing.

HMGB1 is an architectural transcription factor involved in regulation of several promoters, including human β-globin and Bax (Stros et al., 2002; Bianchi and Agresti, 2005). In unchallenged MEFs, activity of several groups of genes, including regulators of cell cycle and apoptosis, has been found to differ between Hmgb1-proficient and -deficient cells (Fig. 6, A and B). Our experiments with cell viability and cell cycle progression support this notion. Therefore, Hmgb1 could either be directly involved in transcriptional regulation or act as a coregulator through interaction with other transcriptional factors (e.g., p53). At present, we expand our studies to other pathways highlighted by DNA microarray analysis.

Because HMGB1 is a DNA bending protein, the role of HMGB1 may consist of active scanning of chromatin, binding to flexible regions of DNA and recruiting other proteins such as p53 and/or regulatory protein kinases. This model does not imply that direct interaction between HMGB1 and p53 is necessary for p53-DNA binding; rather, HMGB1 may change the architecture of DNA and facilitate binding of prebent DNA by p53 (Imamura et al., 2001).

This hypothetical mechanism predicts that abrogation of Hmgb1 functional activity would not affect cellular response to drugs that induce significant alterations in DNA structure. Indeed, no difference in cytotoxic effect was found between $Hmgb1^{+/+}$ and $Hmgb1^{-/-}$ cells treated with cisplatin, a chemotherapeutic agent that introduces sharp kinks in DNA (Wei et al., 2003). Because p53 directly binds to cisplatinated DNA in a non–sequence-specific way, HMGB1 probably is not critical for response to this type of DNA lesion.

Our results indicate that abrogation of Hmgb1 in MEFs reduces apoptotic response to nucleoside analogs and precursors and suggest that decreased Hmgb1 activity due to down-regulated expression or the inactivating mutations can compromise the outcome of chemotherapy. Hmgb1 reveals a complex expression pattern in the mouse brain during development, with a number of cells showing undetectable level of Hmgb1. Moreover, its intracellular localization also varies depending on as-yet-uncharacterized factors (Guazzi et al., 2003). High-resolution mapping of genome imbalance and gene expression profiles of 26 serous epithelial ovarian tumors identified HMGB1 as a gene associated with resistance to chemotherapy (Bernardini et al., 2005). In addition to the regulation of HMGB1 gene expression, the genetic variations in the HMGB1 gene can contribute to variability in drug response. In a recent study of 103 healthy blood donors, six genetic polymorphisms were identified in HMGB1 locus, which may have a regulating role in expression of this protein (Kornblit et al., 2007). Therefore, HMGB1 is a potential target for modulating activity of chemotherapeutic nucleo-

side analogs and precursors. Identification of proteins sensitive to DNA lesions that occur without the loss of DNA integrity provides new insights into the determinants of drug sensitivity in cancer cells.

Acknowledgments

We are grateful to Dr. M. Bianchi for *Hmgb1*$^{+/+}$ and *Hmgb1*$^{-/-}$ cell lines, Drs. K. Helin, M. Oren, T. Taniguchi, B. Vogelstein for their generous gift of plasmids; Ashley Miller, Jennifer Smith, Betty-ann Rogers, Hiren Patel, and Manali Phadke for their excellent technical assistance.

References

An Q, Robins P, Lindahl T, and Barnes DE (2007) 5-fluorouracil incorporated into DNA is excised by the Smug1 DNA glycosylase to reduce drug cytotoxicity. *Cancer Res* **67:**940–945.

Bakkenist CJ and Kastan MB (2003) DNA damage activates ATM through intermolecular autophosphorylation and dimer dissociation. *Nature* **421:**499–506.

Ben-Shaul Y, Bergman H, and Soreq H (2005) Identifying subtle interrelated changes in functional gene categories using continuous measures of gene expression. *Bioinformatics* **21:**1129–1137.

Bernardini M, Lee CH, Beheshti B, Prasad M, Albert M, Marrano P, Begley H, Shaw P, Covens A, Murphy J, et al. (2005) High-resolution mapping of genomic imbalance and identification of gene expression profiles associated with differential chemotherapy response in serous epithelial ovarian cancer. *Neoplasia* **7:**603–613.

Bianchi ME and Agresti A (2005) HMG proteins: dynamic players in gene regulation and differentiation. *Curr Opin Genet Dev* **15:**496–506.

Bolstad BM, Irizarry RA, Astrand M, and Speed TP (2003) A comparison of normalization methods for high density oligonucleotide array data based on variance and bias. *Bioinformatics* **19:**185–193.

Bunz F, Hwang PM, Torrance C, Waldman T, Zhang Y, Dillehay L, Williams J, Lengauer C, Kinzler KW, and Vogelstein B (1999) Disruption of p53 in human cancer cells alters the responses to therapeutic agents. *J Clin Invest* **104:**263–269.

Calogero S, Grassi F, Aguzzi A, Voigtlander T, Ferrier P, Ferrari S, and Bianchi ME (1999) The lack of chromosomal protein hmg1 does not disrupt cell growth but causes lethal hypoglycaemia in newborn mice. *Nat Genet* **22:**276–280.

Carmichael J, DeGraff WG, Gazdar AF, Minna JD, and Mitchell JB (1987) Evaluation of a tetrazolium-based semiautomated colorimetric assay: assessment of chemosensitivity testing. *Cancer Res* **47:**936–942.

Chao C, Hergenhahn M, Kaeser MD, Wu Z, Saito S, Iggo R, Hollstein M, Appella E, and Xu Y (2003) Cell type- and promoter-specific roles of ser18 phosphorylation in regulating p53 responses. *J Biol Chem* **278:**41028–41033.

Decker RH, Levin J, Kramer LB, Dai Y, and Grant S (2003) Enforced expression of the tumor suppressor p53 renders human leukemia cells (U937) more sensitive to 1-[beta-D-arabinofuranosyl]cytosine (ara-C)-induced apoptosis. *Biochem Pharmacol* **65:**1997–2008.

Fernandez-Capetillo O, Lee A, Nussenzweig M, and Nussenzweig A (2004) H2AX: the histone guardian of the genome. *DNA Repair (Amst)* **3:**959–967.

Guazzi S, Strangio A, Franzi AT, and Bianchi ME (2003) HMGB1, an architectural chromatin protein and extracellular signalling factor, has a spatially and temporally restricted expression pattern in mouse brain. *Gene Expr Patterns* **3:**29–33.

Hanasoge S and Ljungman M (2007) H2AX phosphorylation after UV-irradiation is triggered by DNA repair intermediates and is mediated by the ATR kinase. *Carcinogenesis* **28:**2298–2304.

Hock R, Furusawa T, Ueda T, and Bustin M (2007) HMG chromosomal proteins in development and disease. *Trends Cell Biol* **17:**72–79.

Imamura T, Izumi H, Nagatani G, Ise T, Nomoto M, Iwamoto Y, and Kohno K (2001) Interaction with p53 enhances binding of cisplatin-modified DNA by high mobility group 1 protein. *J Biol Chem* **276:**7534–7540.

Jayaraman L, Moorthy NC, Murthy KG, Manley JL, Bustin M, and Prives C (1998) High mobility group protein-1 (HMG-1) is a unique activator of p53. *Genes Dev* **12:**462–472.

Kaeser MD, Pebernard S, and Iggo RD (2004) Regulation of p53 stability and function in HCT116 colon cancer cells. *J Biol Chem* **279:**7598–7605.

Kornblit B, Munthe-Fog L, Petersen SL, Madsen HO, Vindelov L, and Garred P (2007) The genetic variation of the human HMGB1 gene. *Tissue Antigens* **70:**151–156.

Krynetskaia NF, Cai X, Nitiss JL, Krynetski EY, and Relling MV (2000) Thioguanine substitution alters DNA cleavage mediated by topoisomerase II. *FASEB J* **14:**2339–2344.

Krynetski EY, Krynetskaia NF, Bianchi ME, and Evans WE (2003) A nuclear protein complex containing high mobility group proteins B1 and B2, heat shock cognate protein 70, ERp60, and glyceraldehyde-3-phosphate dehydrogenase is involved in the cytotoxic response to DNA modified by incorporation of anticancer nucleoside analogues. *Cancer Res* **63:**100–106.

Krynetski EY, Krynetskaia NF, Gallo AE, Murti KG, and Evans WE (2001) A novel protein complex distinct from mismatch repair binds thioguanylated DNA. *Mol Pharmacol* **59:**367–374.

Longley DB, Harkin DP, and Johnston PG (2003) 5-Fluorouracil: mechanisms of action and clinical strategies. *Nat Rev Cancer* **3:**330–338.

Lorenz M, Hillisch A, Payet D, Buttinelli M, Travers A, and Diekmann S (1999) DNA bending induced by high mobility group proteins studied by fluorescence resonance energy transfer. *Biochemistry* **38:**12150–12158.

Maybaum J and Mandel HG (1983) Unilateral chromatid damage: a new basis for 6-thioguanine cytotoxicity. *Cancer Res* **43:**3852–3856.

McKinney K, and Prives C (2002) Efficient specific DNA binding by p53 requires both its central and C-terminal domains as revealed by studies with high-mobility group 1 protein. *Mol Cell Biol* **22:**6797–6808.

Meek DW (2004) The p53 response to DNA damage. *DNA Repair (Amst)* **3:**1049–1056.

Rich TA, Shepard RC, and Mosley ST (2004) Four decades of continuing innovation with fluorouracil: current and future approaches to fluorouracil chemoradiation therapy. *J Clin Oncol* **22:**2214–2232.

Rogakou EP, Nieves-Neira W, Boon C, Pommier Y, and Bonner WM (2000) Initiation of DNA fragmentation during apoptosis induces phosphorylation of H2AX histone at serine 139. *J Biol Chem* **275:**9390–9395.

Sahasrabudhe PV, Pon RT, and Gmeiner WH (1996) Solution structures of 5-fluorouracil-substituted DNA and RNA decamer duplexes. *Biochemistry* **35:**13597–13608.

Seibert E, Osman R, and Ross JBA (2005) Dynamics of DNA damage recognition, in *DNA Damage Recognition* (Siede W, Kow YW, and Doetsch PW eds) pp 3–19, Taylor and Francis, New York.

Somerville L, Krynetski EY, Krynetskaia NF, Beger RD, Zhang W, Marhefka CA, Evans WE, and Kriwacki RW (2003) Structure and dynamics of thioguanine-modified duplex DNA. *J Biol Chem* **278:**1005–1011.

Soubeyrand S, Schild-Poulter C, and Hache RJ (2004) Structured DNA promotes phosphorylation of p53 by DNA-dependent protein kinase at serine 9 and threonine. *Eur J Biochem* **271:**3776–3784.

Stros M, Ozaki T, Bacikova A, Kageyama H, and Nakagawara A (2002) HMGB1 and HMGB2 cell-specifically down-regulate the p53- and p73-dependent sequence-specific transactivation from the human Bax gene promoter. *J Biol Chem* **277:**7157–7164.

Wei M, Burenkova O, and Lippard SJ (2003) Cisplatin sensitivity in Hmbg1−/− and Hmbg1+/+ mouse cells. *J Biol Chem* **278:**1769–1773.

Xie H, Midic U, Vucetic S, and Obradovic Z (2007) Algorithmic methods for the analysis of gene expression data, in *Handbook of Applied Algorithms: Solving Scientific, Engineering and Practical Problems* (Nayak A and Stojmenovic I, eds), in press, John Wiley & Sons, Inc.

Yamada S and Maruyama I (2007) HMGB1, a novel inflammatory cytokine. *Clin Chim Acta* **375:**36–42.

Yin B, Kogan SC, Dickins RA, Lowe SW, and Largaespada DA (2006) Trp53 loss during in vitro selection contributes to acquired ara-c resistance in acute myeloid leukemia. *Exp Hematol* **34:**631–641.

Zhang L, Yu J, Park BH, Kinzler KW, and Vogelstein B (2000) Role of BAX in the apoptotic response to anticancer agents. *Science* **290:**989–992.

Zhang X, Jeffs G, Ren X, O'Donovan P, Montaner B, Perrett CM, Karran P, and Xu YZ (2007) Novel DNA lesions generated by the interaction between therapeutic thiopurines and UVA light. *DNA Repair (Amst)* **6:**344–354.

Address correspondence to: Evgeny Krynetskiy, Temple University School of Pharmacy, 3307 North Broad Street Philadelphia, PA 19140. E-mail: ekrynets@temple.edu